

Short-chain dehydrogenase/reductase 3 (DHRS3) deficiency results in altered patient retinoid profiles

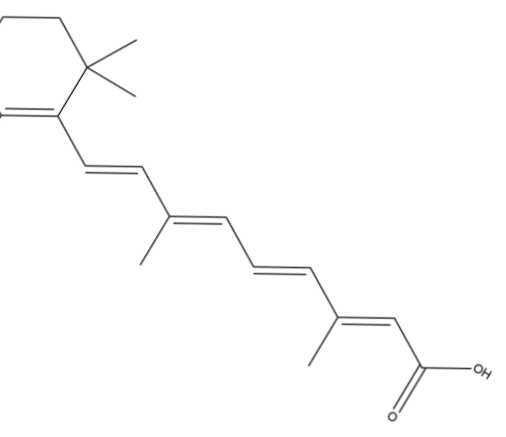
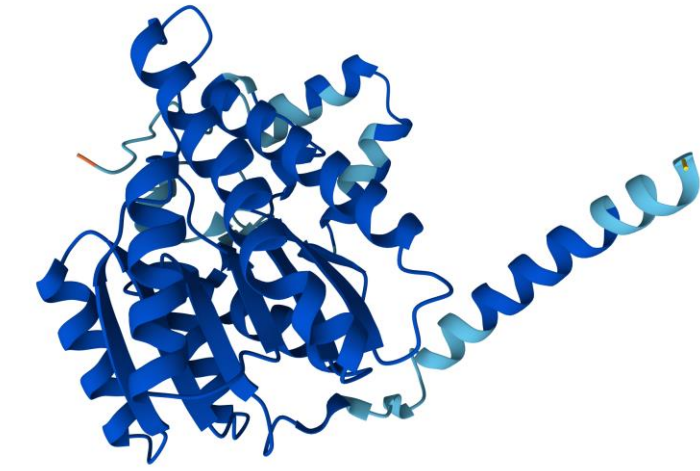
Jianshi Yu¹, Christina Williams¹, Tian Liu¹, Nageswara Pilli¹, Paul A. Trainor², Alexander A. Moise³, Andrew Wilkie⁴, Maureen A. Kane¹

¹ Department of Pharmaceutical Sciences, School of Pharmacy, University of Maryland, Baltimore, MD, 21201, USA

² Stowers Institute for Medical Research, Kansas City, MO, United States; University of Kansas Medical Center, Department of Anatomy and Cell Biology, Kansas City, KS, United States.

³ Northern Ontario School of Medicine, Biomolecular Sciences Program and Department of Chemistry and Biochemistry, Laurentian University, Sudbury, ON, P3E 2C6, Canada

⁴ Clinical Genetics Group, Weatherall Institute of Molecular Medicine, University of Oxford, Oxford, UK



Background

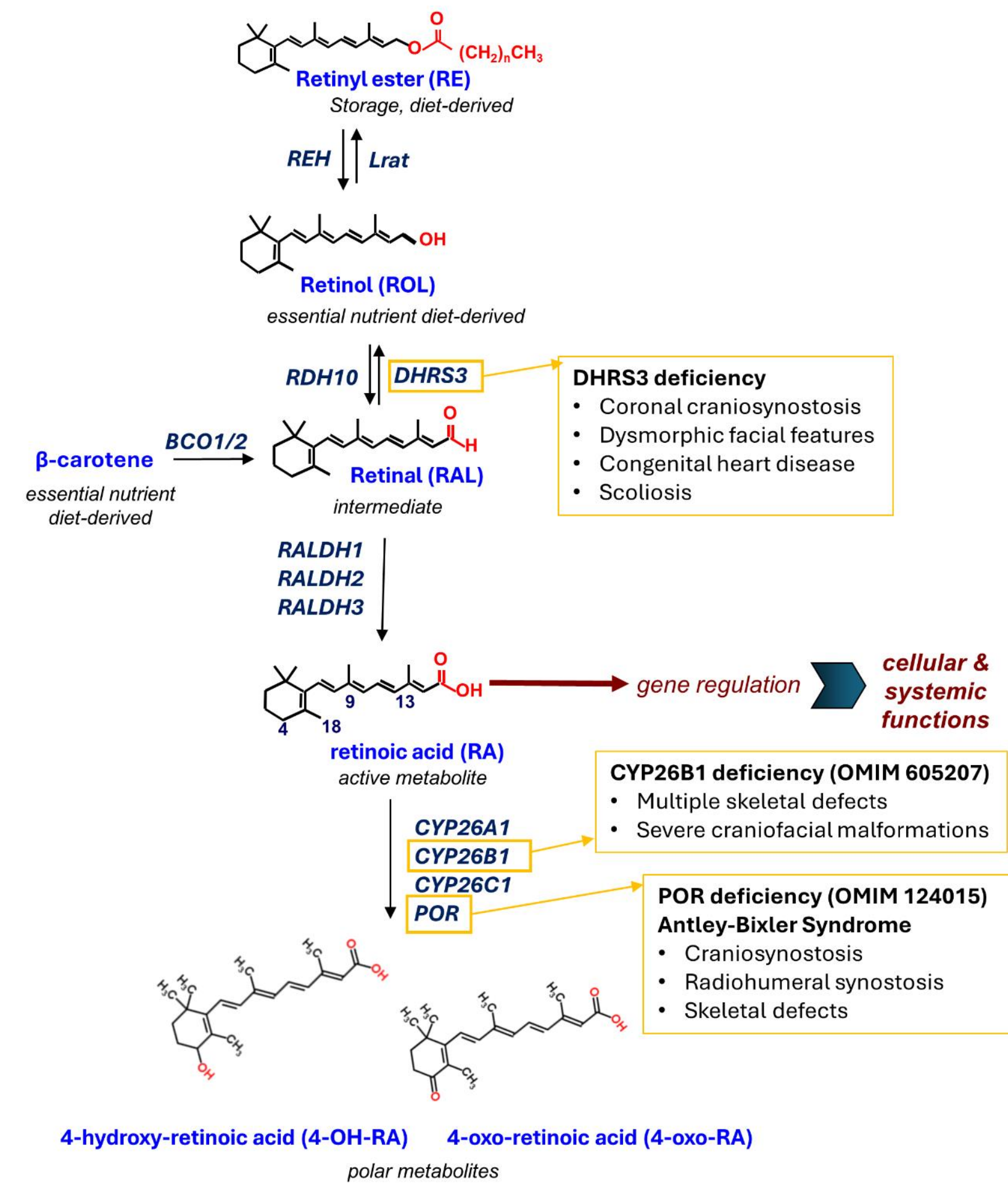


Figure 1. Schematic of RA metabolism and related human congenital disorders. All-trans retinoic acid (RA), the active metabolite, is obligatorily derived from two dietary sources, ROL (vitamin A) and β -carotene (pro-vitamin A) and derivatives. Oxidation of RAL, the intermediate metabolite from both these sources, to RA occurs irreversibly, whereas oxidation of ROL to RAL is reversible, being catalysed by related SDR16C enzymes RDH10 and DHRS3. Note that excess ROL is stored as RE. Breakdown of RA is mediated by three cytochrome P450 enzymes CYP26A1, CYP26B1 and CYP26C1, which all require POR as a universal electron donor. Previously identified genetic disorders of RA metabolism are indicated inside the yellow boxes.

Signaling by the morphogen all-trans-retinoic acid (RA) is critical for embryonic development, during which its tissue concentration needs to be tightly regulated. RA regulation is complex and includes enzymes involved in the metabolism of retinol into RA. Conversion of retinol to RA involves two successive oxidation steps where the oxidation of retinol to retinaldehyde is rate-limiting and reversible and therefore represents the major regulatory point during synthesis. The forward reaction is catalysed by several retinol dehydrogenases including, most critically for embryogenesis, RDH10 whereas dehydrogenase/reductase 3 (DHRS3; also named SDR16C1) is the major embryonic enzyme catalysing the opposite reaction (retinaldehyde to retinol).

Two previously reported recessively inherited clinical disorders that are attributable to RA excess

- Deficiency of *CYP26B1*, encoding one of the three cytochrome P450-dependent enzymes that are key for retinoic acid catabolism [1]
- Antley-Bixler syndrome caused by biallelic variants in the *POR* gene encoding cytochrome P450 oxidoreductase, the universal electron donor for all microsomal P450 enzymes, including *CYP26B1* [2]

DHRS3 deficiency: We recently defined a novel developmental syndrome associated with biallelic hypomorphic variants in *DHRS3* [3]

- Deletion of the promoter and 5'-untranslated region (UTR) of *DHRS3* and a missense variant p.(Val171Met) were pathogenic with reduced DHRS3 activity in vitro and in vivo
- Three additional homozygous missense variants of *DHRS3* [p.(Val110Ile), p.(Gly115Asp), p.(Glu244Gln)] had effects on DHRS3 activity did not meet the threshold to assign likely pathogenicity

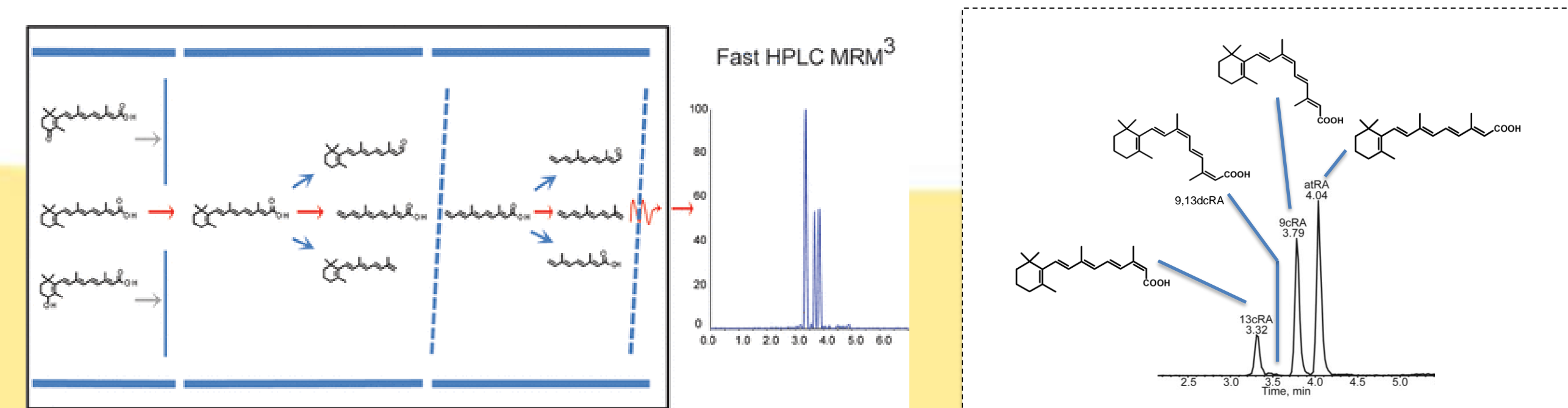
Objective

Direct quantification of the endogenous retinoid profile in patient plasma to assess DHRS3 mutations.

Methods

Quantification of retinoid metabolites in patient samples

- Blood was collected in EDTA tubes and plasma separated by centrifugation at 4°C, under conditions designed to minimize exposure to ultraviolet light. Plasma was stored in 0.2 ml aliquots at -80°C until analysis. Extraction of retinoids was performed using 100-200 μ L of plasma in each replicate with multiple aliquots independently extracted and analyzed from each patient.
- Extraction was performed under yellow lights using a two-step liquid-liquid extraction, with 4,4-dimethyl-RA as an internal standard for RA and retinyl acetate as an internal standard for ROL and total RE. [4-8] All authentic retinoid standards were obtained from Sigma-Aldrich except 4,4-dimethyl-RA, which was obtained from Toronto Research Chemicals. Concentrations of RE and ROL were determined using high performance liquid chromatography with ultraviolet spectroscopy (HPLC-UV) with an ACQUITY H-Class Ultra-HPLC equipped with a photodiode array (PDA) detector (Waters, Milford, MA). [5,6] Concentrations of RA were determined using liquid chromatography-multistage tandem mass spectrometry (LC-MS/MS) using atmospheric pressure chemical ionization in positive-ion mode with a 6500+ QTRAP hybrid tandem quadrupole mass spectrometer (AB Sciex, Foster City, CA). [4]
- Plasma retinoids are expressed as moles per milliliter of plasma and shown as mean \pm standard deviation (SD) of measurements of individual aliquots from a given patient. Retinoid levels in patients were compared to levels in unaffected relatives, and in some cases unrelated controls from the same geographic area, using a one-way ANOVA with Tukey's correction for multiple testing in GraphPad Prism V6.07.
- Notional reference interval ranges for each family as a subpopulation that define excess and deficiency were calculated using the % critical difference in Soderlund et al. [9] and the average wild-type (WT) levels in each family subpopulation. If WT were not available in a family subpopulation, average levels in heterozygotes were used as the control to determine the notional reference interval of the family subpopulation



Results

Figure A / B. Measurement of endogenous retinoids in plasma of individuals from Families 1, 2, 3 and 5.

A, ROL (nmol/ml) as determined by HPLC-UV.

B, RA (pmol/ml) as determined by LC-MS/MS.

- The x-axis labels indicate the identity of the individual analysed (see pedigrees in Fig S1), and below, whether they are wild-type (WT), heterozygous (Het) or homozygous (Hom) for the corresponding DHRS3 variant. Additional unrelated WT controls C1-C4 were included in the analyses of Families 1 or 3.

- Limits for excess and deficiency (parallel blue lines) were calculated for each family as a subpopulation using the average WT (dashed lines) or average Het (dotted lines) levels and the critical difference from Soderlund et al.[9]

- In part A, plasma retinol levels that define vitamin A deficiency (VAD, 0.7 nmol/mL) and low vitamin A status (0.7-1.05 nmol/mL) are notated on the y-axis. [10]

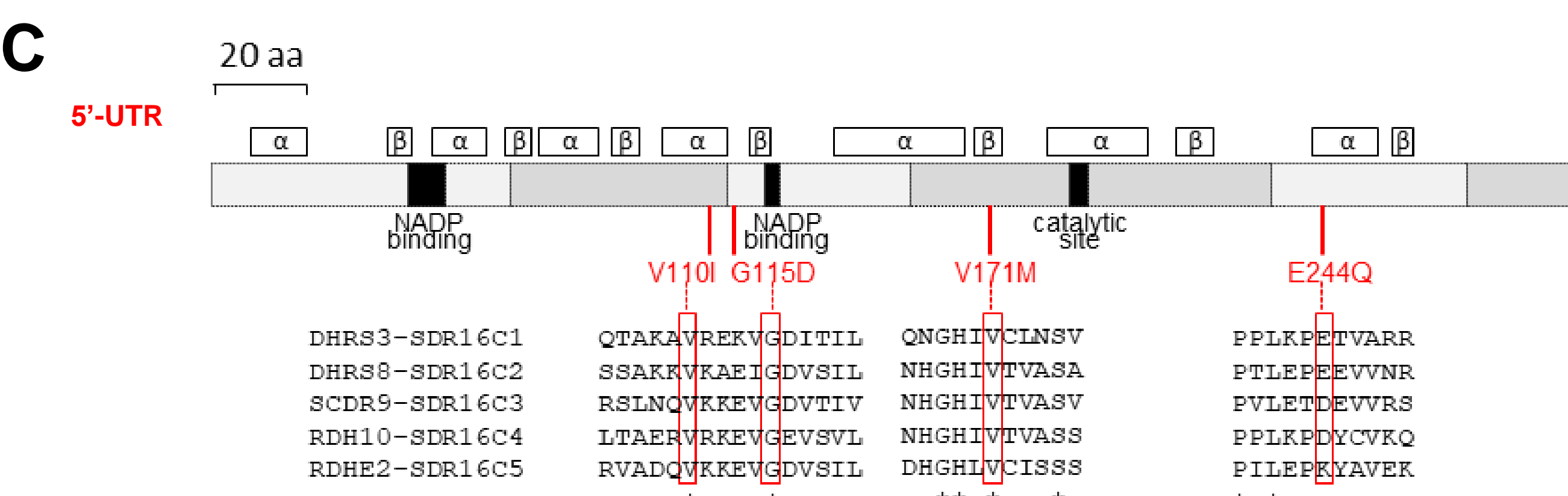
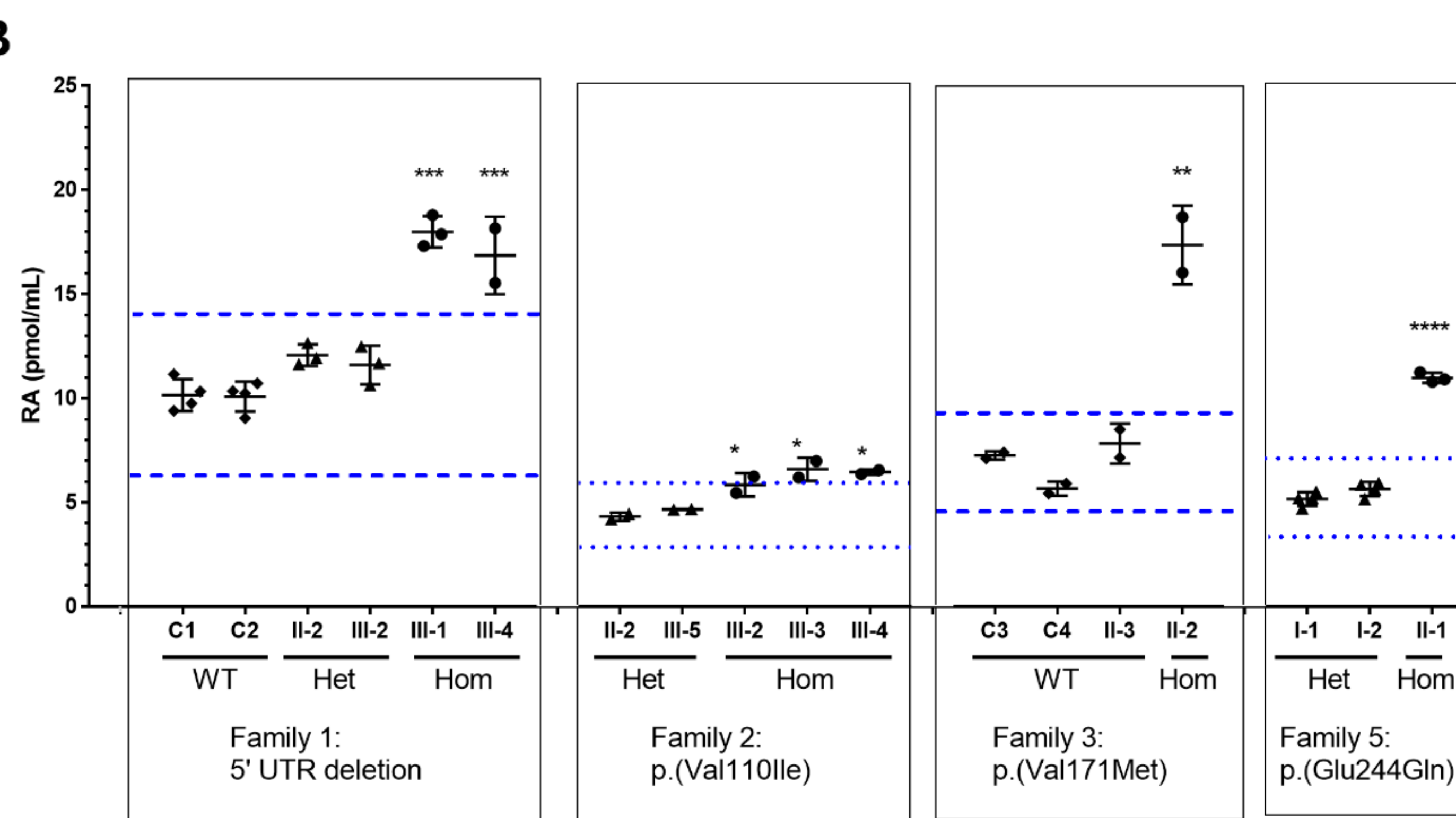
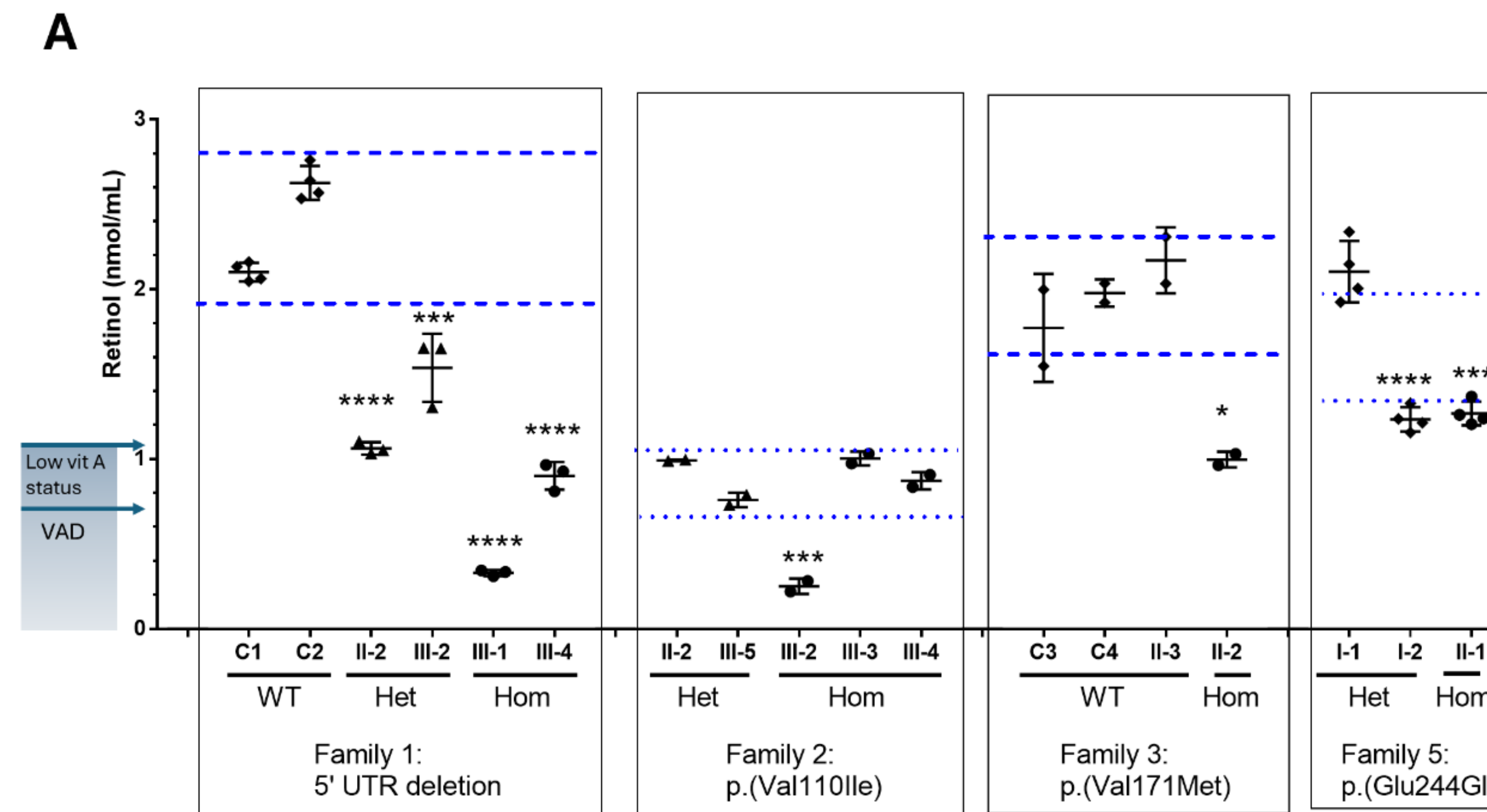
- Significance of differences of Hom cases within individual families, compared to unaffected individuals, were determined by one-way ANOVA with Tukey's correction for multiple comparisons. * $p < 0.05$, ** $p < 0.01$, *** $p < 0.001$, **** $p < 0.0001$.

- Hom individuals have elevated RA levels that were above of the threshold for excess as defined according to the reported critical difference at the 95% confidence level [9]

Figure C. Structure of DHRS3 and encoded protein and location of homozygous variants. Cartoon of protein. Alternating grey blocks of different shades indicate regions encoded by sequential exons. Black segments show regions involved in enzymatic functions. Above the cartoon are shown regions predicted by AlphaFold to adopt either α -helix or β -sheet structure with a per-residue confidence score >90 . Below the cartoon, the locations of the four amino acid substitutions are shown with local alignments of the five members of the human SDR16C family (red rectangles). [11] Asterisks denote invariant amino acids. Note that DHRS8 and SCDR9 are synonymous with HSD17B11 and HSD17B13, respectively.

Table A. Features of homozygous variants of DHRS3 assessed in this work

Family #	1	2	3	5
Mutation	5'-UTR deletion	p.(Val110Ile)	p.(Val171Met)	p.(Glu244Gln)
Location	UK/Pakistan	Jordan	Spain	German/Syria
The nutrient production adequacy [12]	0.8	0.5	1.3	1.1
Pathogenicity	Pathogenic	Likely benign	Pathogenic	"hot" VUS (variant of uncertain significance)
Craniofacial	Craniosynostosis, Hypertelorism, broad nasal bridge, bulbous nasal tip, short palpebral fissures		Craniosynostosis, Hypertelorism, proptosis, mild microcephaly	Macrocephaly, severe hypertelorism, R cleft lip, L cleft palate
Developmental delay/Intellectual disability	Normal/ Moderate	Moderate	Mild	Severe
Brain imaging	Normal/Ventricular dilatation, Cerebellar vermis hypoplasia	NA	NA	NA
Cardiac	Atrial septal defect/ Atrial septal defect, patent foramen ovale		Aortic pseudo-coarctation/root dilatation, absent pericardium	
Additional features	Psoriasis, vesicular milia-like lesions on either side of the nose, long fingers, / Bilateral cryptorchidism, hypospadias, long fingers, persistent feeding difficulties requiring nasogastric tube feeding, bilateral conductive hearing impairment, disordered breathing during sleep		Right inguinal hernia, mild conductive hearing impairment	Short stature, epilepsy, severe visual impairment with divergent strabismus and nystagmus



Results

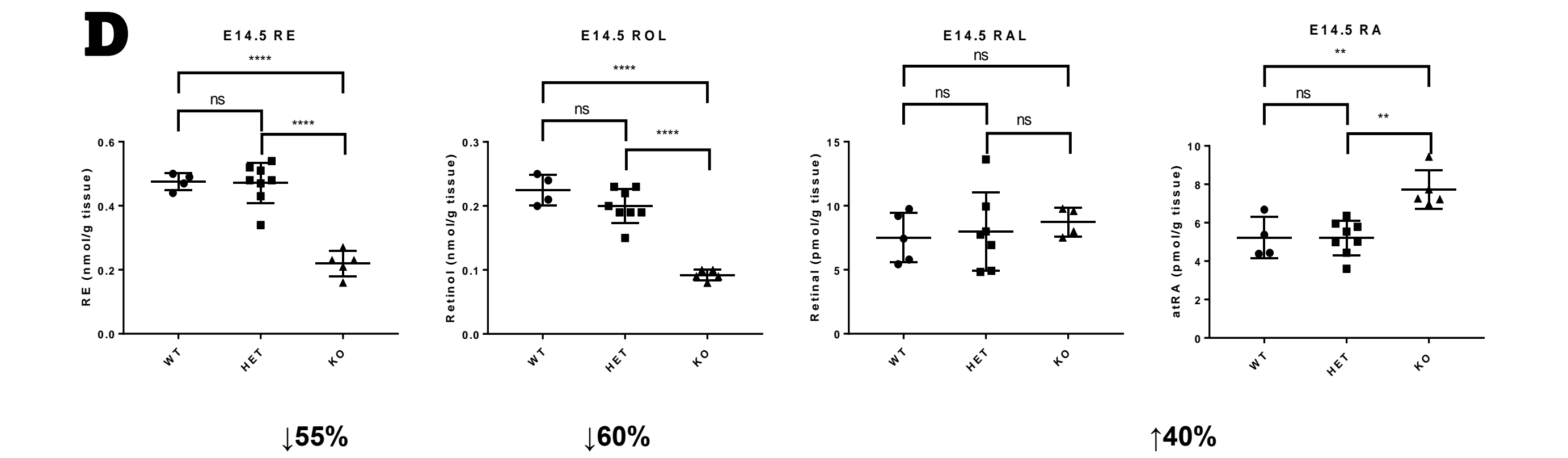


Figure D. Alterations in the levels of retinoid metabolites as a result of Dhhrs3-deficiency in mouse. Global levels of all-trans-retinol, retinyl esters, and ATRA were analyzed in WT, Dhhrs3^{+/-} (Het), or Dhhrs3^{-/-} (KO) mice. E14.5 embryos were derived from dams maintained on a VAS diet. Retinoids were extracted from whole embryos and analyzed using LC-UV in the case of all-trans-retinol, retinaloximes, and retinyl esters and LC-MS/MS in the case of ATRA. Amount of each retinoid was normalized based on the weight of embryonic tissue. Data represent means \pm SD of retinoid levels from 4-5 embryos/genotype; * $P < 0.05$, *** $P < 0.001$ vs. WT; ## $P < 0.01$, ### $P < 0.001$ vs. Het. [13]

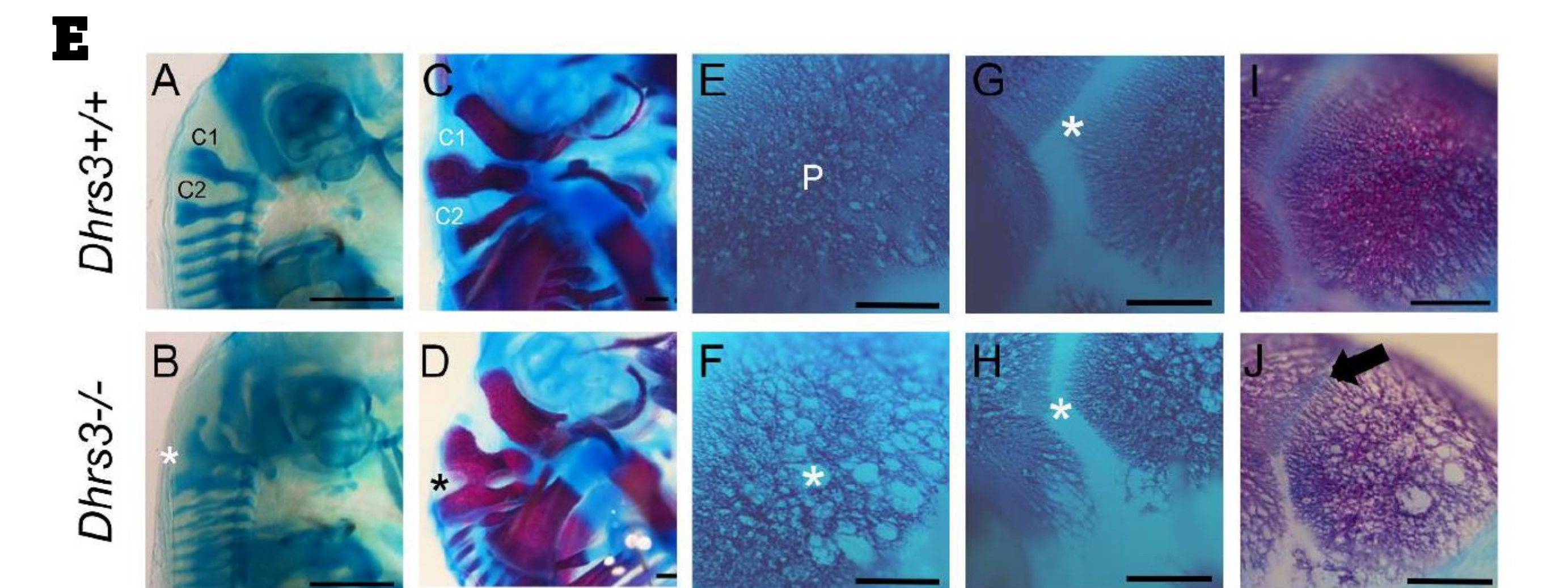


Figure E. Dhhrs3^{-/-} mutant mice exhibit axial and cranial skeletal anomalies. A-B, Alcian blue staining of cartilage reveals distinctive C1 and C2 vertebrae in E14.5 Dhhrs3^{+/-} mouse embryos, and their fusion (white asterisk) in Dhhrs3^{-/-} embryos, which is consistent with upregulated RA signaling during embryogenesis. C-D, Alizarin red and Alcian blue staining of bone and cartilage respectively illustrates the more pronounced fusion (black asterisk) of C1 and C2 in Dhhrs3^{-/-} embryos compared to Dhhrs3^{+/-} embryos. E-F, Alizarin red staining of the parietal (P) bone reveals less dense and more porous bone (white asterisk) in Dhhrs3^{-/-} embryos compared to Dhhrs3^{+/-} embryos. G-I, Alizarin red staining of the calvaria illustrates the narrowing of the coronal suture (white asterisk) and ectopic bone growth (black arrow) into the coronal suture in Dhhrs3^{-/-} embryos compared to Dhhrs3^{+/-} embryos. Scale bars 500 μ m.

Conclusions

- Quantification of the endogenous retinoid profile in patient plasma showed plasma from homozygous patients had significantly reduced retinol and elevated RA, compared to controls and carrier relatives.
- Five of the individuals (harboring two different variants) display features consistent with a novel retinoic acid embryopathy.
- Shared phenotypes include craniosynostosis, scoliosis and structural heart defects, features congruent with further phenotyping of the mouse Dhhrs3^{-/-} model.
- These data help define regulatory factors and enrich our understanding of RA homeostasis in vivo.

Bibliography

- [1] Laue K et al. (2011) *Am J Hum Genet* 89:595-606
- [2] Fluck CE, et al. (2004) *Nat Genet* 36:228-230.
- [3] Hashimoto AS, Yu J, Williams C et al. ...Trainor PA, Moise AR, Wilkie OM, Kane MA (2024) *Genetics in Medicine Open*, Submitted.
- [4] Jones, Yu, Pierzchalski, & Kane, Anal. Chem. 2015, 87, 3222
- [5] Kane & Napoli, *Methods Mol Biol*, 2010, 652, 1-54
- [6] Kane et al. *Anal. Biochem.* 2008, 378, 71-79.
- [7] Kane et al., *Anal. Chem.*, 2008, 80, 1702-1708;
- [8] Kane et al., *Biochem J.*, 2005, 380, 363-369.
- [9] Soderlund MB, et al. (2002) *Scand J Clin Lab Invest* 62:511-519.
- [10] West KP, Jr. (2002) *J Nutr* 132: 2857S-2866S.
- [11] Lundova T et al. *Chem Biol Interact* (2015) 234: 178-187.
- [12] Chen C, et al. (2021) *Front Nutr* 8:739755.
- [13] Billings et al. (2013) *FASEB J.* 27:4877-89.

Funding

National Institutes of Health, Eunice Kennedy Shriver National Institute of Child Health and Human Development grant no. R01HD077260 and Internal Pilot Funds from the University of Maryland School of Pharmacy. Additional support was provided by the University of Maryland School of Pharmacy Mass Spectrometry Center (SOP1841-IQB2014).